ELSEVIER

Materials Characterization 45 (2000) 221–226

MATERIALS CHARACTERIZATION

Characterization of alumina ceramics by ultrasonic testing

L.-S. Chang[a,*], T.-H. Chuang[b], W.J. Wei[b]

[a]*Institute of Materials Engineering, National Chung Hsing University, 250 Kuo Kuang Road, Taichung 40227, Taiwan*
[b]*Institute of Materials Science and Engineering, National Taiwan University, Taipei 106, Taiwan*

Received 11 April 1999; received in revised form 8 June 2000; accepted 8 June 2000

Abstract

Some material characteristics of alumina ceramics, e.g., porosity, Young's modulus and Poisson's ratio, have been evaluated using ultrasonic sound. Experimental results showed that the velocity of an ultrasonic sound wave in alumina ceramics decreased proportionally with increasing porosity. Young's modulus and Poisson's ratio calculated from the longitudinal and transverse ultrasonic velocities were found to be dependent on porosity. The results from the present program have been compared with data from the literature, and similarities and differences discussed. The deviation of these data from a theoretical prediction may be due to the texture of the porosity introduced by different alumina-forming processes.

Keywords: Alumina; Ceramics; Ultrasonic

1. Introduction

Recently, refined ceramics have been widely researched as potentially important engineering materials because of their elevated melting points, high strength/density ratios and excellent corrosion resistance. However, comprehensive evaluation of their properties and microstructures is complicated, especially when destructive types of testing are involved. The physical nature of ceramics often leads to a lack of reproducibility in the data produced in conventional mechanical tests. This must be countered first by developing reliable methods of preparing consistent sets of samples. Then, because of the lack of data reproducibility (i.e., a low Weibull coefficient), large numbers of samples must be prepared and tested in order to reduce the uncertainty of the results. In contrast, nondestructive testing promises a useful solution to these problems [1], such that a specimen can be examined repeatedly until the test is fully satisfied.

Nondestructive test methods include penetrant testing, Eddy current testing, magnetic evaluation, X-ray evaluation and ultrasonic testing. Ultrasonic testing can be used not only in detecting cracks, holes and inclusions, but also in evaluating material characteristics such as density, texture and mechanical properties. In addition, there are fewer limitations on the size and shape of samples required in this easily performed method.

Our previous work, which was dedicated to the theoretical and experimental analysis of the artificial defects in alumina, demonstrated the application of ultrasonic testing in the evaluation of ceramics [2]. The present work was planned to investigate the velocity of various ultrasonic sound waves with respect to the material characteristics of alumina. Those characteristics involve the porosity, the Young's modulus and the Poisson's ratio of several alumina materials.

* Corresponding author. Tel.: +886-4-280500 ext. 714; fax: +886-4-2857017.

E-mail address: lschang@dragon.nchu.edu.tw (L.-S. Chang).

1044-5803/00/$ – see front matter
PII: S1044-5803(00)00081-4

2. Theory

In a sound medium, the velocity of wave transport from some point to a neighboring location depends on the interaction, point mass and medium structure. Elastic theory indicates that sound wave velocities in an infinitely large solid medium can be expressed as a function of Young's modulus (E), shear modulus (G), density (ρ) and Poisson's ratio (ν) [3]. The relationships are shown below:

1. Longitudinal wave velocity

$$v_l = \sqrt{\frac{E(1-\nu)}{\rho(1+\nu)(1-2\nu)}} \tag{1.1}$$

2. Transverse wave velocity

$$v_t = \sqrt{\frac{G}{\rho}} = \sqrt{\frac{E}{2\rho(1+\nu)}} \tag{1.2}$$

In order to solve Eqs. (1.1) and (1.2), we define $r = v_l/v_t$, which leads to (Eq. (2.2)):

$$\nu = \frac{r^2-2}{2(r^2-1)} \tag{2.1}$$

$$E = \frac{\rho v_t^2(3r^2-4)}{r^2-1} \tag{2.2}$$

Relationships have been reported between sound velocity and porosity [4,5]. Sayers [4] noted that if closed holes in a material are spherical, the change of longitudinal sound velocity (v) due to the presence of the holes is approximately proportional to the porosity p of the material. This can be written as follows:

$$\frac{v}{v_l} = 1 + Ap \tag{3}$$

where A is a dimensionless constant. For alumina, A is -0.56.

Phani [5] developed a series of equations for the interpretation of the relationship of sound velocity to cylindrical pores [6]. The longitudinal and transverse velocity of the equations can be written as

$$v_l = \sqrt{\frac{K_{23}^* + G_{23}^*}{\rho_0(1-p)}} \tag{4.1}$$

$$v_t = \sqrt{\frac{G_{23}^*}{\rho_0(1-p)}} \tag{4.2}$$

in which K_{23}^* and G_{23}^* are dependent on porosity, Poisson's ratio and bulk and shear modulus of nonporous material. From Phani's viewpoint, the G_{23}^* property depends on the critical porosity, at which a transition in phase contiguity occurs. This critical porosity value, in turn, depends on the manufacturing process. However, G_{23}^* was defined with the upper- and lowerbounds in the original work concerning the theory of cylindrical pores [7].

From the simple linear density dependence of sound velocity (Eq. (3)), the Young's modulus of a porous material can be written as a function of porosity [7,8]:

$$E = \sum_{i=0}^{5} m_i p^i \Big/ \sum_{i=0}^{2} n_i p^i \tag{5}$$

where the coefficients m_i and n_i are the function of bulk density and the coefficient A in Eq. (3) for the longitudinal and transverse waves.

The following equations, recently proposed by Sudduth [9], in general, represent the relationship between Young's modulus and porosity. If $\sigma \neq 1$ (Eq. (6.1)),

$$\ln\left(\frac{E}{E_0}\right) = \frac{[E]p_i}{\sigma-1}\left[\left(\frac{p_i-p}{p_i}\right)^{1-\sigma} - 1\right] \tag{6.1}$$

or $\sigma = 1$ (Eq. (6.2))

$$\ln\left(\frac{E}{E_0}\right) = -[E]p_i \ln\left(\frac{p_i-p}{p_i}\right) \tag{6.2}$$

where E is the Young's modulus of a porous polycrystalline solid, E_0 is the Young's modulus of a non-porous polycrystalline solid, $[E]$ is an intrinsic modulus, σ is the porosity interaction coefficient and p_i is an intrinsic porosity. The intrinsic porosity is a critical value at which Young's modulus of the porous solid approaches zero. For this generalized equation, some empirical results [10–12] can be formulated within the scope of the interaction coefficient.

3. Experimental procedure

3.1. Preparation of alumina samples

Alumina specimens were prepared using a colloidal process to obtain the specimens containing various characteristics. The raw material was alumina powder produced by the Aluminum Company of

Table 1
Compositions of the alumina ceramic powder (Alcoa A16-SG)

Compositions	A16-SG
Al_2O_3	99.7
SiO_2	0.025
ZrO_2	...
TiO_2	...
MgO	0.05
Fe_2O_3	0.01
Na_2O	0.08
Crystalline phase	α-Al_2O_3
Specific surface area	9

America (Alcoa A16-SG, USA). The impurity contents are listed in Table 1. In the colloidal process, the alumina powder was added into a water solution containing a dispersant, 0.5 wt.% Darvan C (R.T. Vanderblit, CT, USA), to prepare a slurry with a 50 wt.% solid content. The slurry was ball-milled for 48 h to produce a well-dispersed slurry. This homogeneously mixed alumina slurry was pressure-cast to form green cakes of 25-mm diameter and 10-mm thickness. The casting pressure was maintained at 10 kg/cm^2. The green cake was dried at 60°C in an air furnace for 24 h.

The alumina was sintered in an air furnace for 2 h at the temperatures between 1250°C and 1550°C to produce alumina specimens with different densities. Sintering at 1550°C for 2 h produced an almost fully dense alumina sample. The bulk density (ρ) of each sintered samples was measured by means of the Archimedes' method [13]. The porosity of the samples was calculated from the bulk density with the value 4.0 g/cm^3 for fully dense alumina ($p=1-\rho/4$). The surfaces of the sintered specimens were ground using a 500-mesh# diamond grinding wheel with a grinding rate of 0.02–0.04 mm/cycle to ensure a flat surface in order to ensure good contact between the specimens and the transducer.

3.2. Ultrasonic testing of alumina

The testing instrument included an ultrasonic USIP 12 unit, a thickness meter DTM 12, and a high-frequency generator USH 100 (Krautkramer-Branson, FRG). The transducers included longitudinal and transverse types of which the frequencies 5, 10 and 50 MHz were used. Glycerin and SWC were chosen as the couplants between the specimen and transducer, depending on the different viscosity and resonance requirements for the longitudinal transducer or the transverse transducer. Ultrasonic testing was performed using the one-transducer-pulse method in the A-scan mode (point mode). The sound velocity was calculated by observing the time difference (t) between two back-reflected pulses and measuring the thickness (d) using the DTM 12. The velocity (v) equals $2d/t$. Measurement accuracy was within 1%.

4. Results and discussion

4.1. Porosity effect

Fig. 1 shows the relationship between the longitudinal sound velocity and the porosity of alumina specimens at 5, 10 and 50 MHz, while Fig. 2 represents the relationship between the transverse velocity and the porosity at 5 and 10 MHz. It can easily be seen that the sound velocity is inversely proportional to the specimen porosity, i.e., the higher the porosity, the slower the sound wave propagates. The linear relationship between the sound velocity and the porosity derived from previous equations was indicated in Figs. 1 and 2. Similar results have also been obtained [14,15]. There are no apparent differences between the results from various frequencies, indicating a lack of frequency dependence. This is in agreement with the observations of Bridge et al. [16] that the sound velocity does not change at the frequencies higher than 1 MHz.

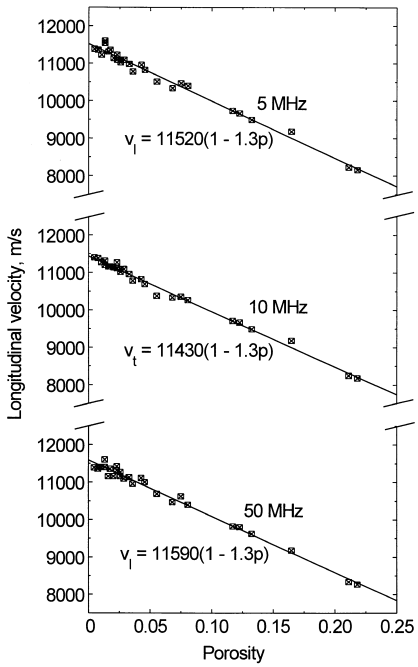

Fig. 1. Relationship between the longitudinal sound wave velocity and the porosity of alumina tested at 5, 10 and 50 MHz.

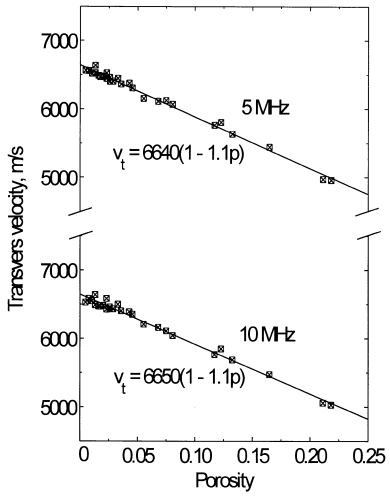

Fig. 2. Relationship between the transverse sound wave velocity and the porosity of alumina tested at 5 and 10 MHz.

From the linear fitting of the experimental data in Fig. 1 and Fig. 2, we obtain

$$v_l = C_1(1 - 1.3p) \tag{7.1}$$

$$v_t = C_2(1 - 1.1p) \tag{7.2}$$

where C_1 is 11520, 11430 and 11590 m/s for 5, 10 and 50 MHz, respectively, and C_2 is 6640 and 6650 m/s for 5 and 10M Hz, respectively. The value (-1.3) of the factor A in Eq. (7.1) is approximately twice the theoretical value of -0.56 calculated from the model system containing spherical pores. One of the possible explanations of this difference is the interconnection between the pores that would result with cylindrical-like pores [17].

In order to resolve the argument, we compare our results with those of the model system containing cylindrical pores, as the lines drawn in Fig. 3. The data points with and without crosses are our experimental data and those from Nagarajan [18], respectively. The solid line was plotted according to Eqs. (4.1) and (4.2) (from Ref. [5]). The plot also contains the upper- and lowerbounds (dashed lines) defined by Hashin and Rosen [6]. The values of the parameters for calculating these lines are: bulk modulus = 290 GPa, shear modulus = 172 GPa and Poisson's ratio = 0.25. It was found that our data on the longitudinal wave lie closest to the lowerbound line but our data on the transverse wave fall between the solid line and the lowerbound line. This indicates that the Poisson's ratio, assumed to be constant in the equations, may actually be strongly dependent on porosity. That implies that the distribution of pores in the matrix may be anisotropic. Such microstructural anisotropy may result from the forming process (uniaxial filtration). The relationship between Poisson's ratio and porosity will be discussed later.

Pore anisotropy provides an adequate explanation for the porosity dependence of Poisson's ratio. However, actual microstructural observation of the pore structure is almost impossible in the present case. The average particle size of the alumina powder is about 0.3 μm. That means the pore size is less than 0.1 μm in green cake and even 0.01 μm in a sintered bulk. These fine pores are easily destroyed during polishing by the normal methods. Even if the pore size could be measured, the pore shape and structure, which are more important than the pore size in this case, are undeterminable.

4.2. Young's modulus and Poisson's ratio

Introducing the linear relationship between the ultrasonic velocity and porosity of Eqs. (7.1) and (7.2) into Eq. (5), we obtain (Eq. (8)):

$$E = \frac{3.87 - 23.7p + 57.3p^2 - 68.9p^3 + 41.1p^4 - 9.7p^5}{8.81 - 24.7p + 17.0p^2} \tag{8}$$

(E is in units of 10^3 GPa). The calculated Young's modulus is normalized and plotted as a function of porosity, as shown in Fig. 4, in which the dashed lines are calculated from Eq. (3).

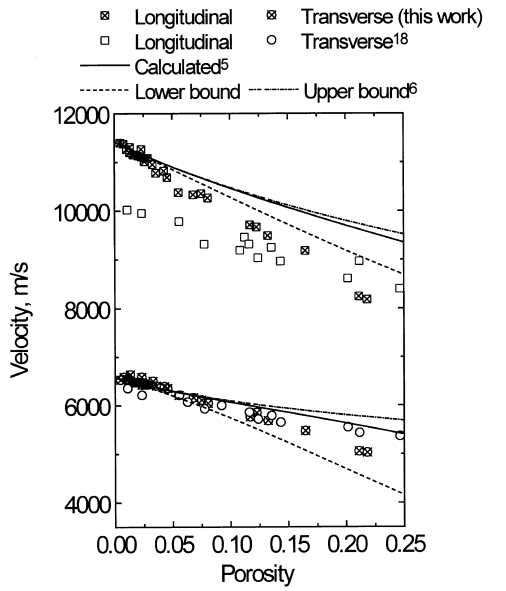

Fig. 3. Comparison between the experimental data of the sound velocity obtained in this work and those from the literature plotted as a function of porosity.

Fig. 4 compares the Young's modulus prediction curve from the present work with values from various sources in the literature [5,6,10,18–25]. Good agreement is noted between the calculated value in this work (thick solid line) and the lowerbound calculated in Ref. [6]. The dotted line from Gatto [19], whose results were also obtained from measurements of sound velocity, falls close to our data. Additionally, the calculated curve in this work can qualitatively describe most of the experimental data from the literature. Conversely, the calculated line from Phani [5], the upperbound line [6] and the points from Refs. [18,20] deviate noticeably from our calculated line. This difference may derive from the forming process of the alumina sample. The experimental data that are in agreement with our own data are from specimens formed by a uniaxial forming method, e.g., cold pressing [21,22], hot pressing [11,22,23], extrusion [24,25] and pressure casting (this work). However, the other data, which are in poor agreement with our own, were obtained from specimens prepared either by isostatic pressing [18] or slip-casting [20]. We believe that the uniaxial pressure induces a pore texture in which the density distribution is anisotropic, i.e., the porosity is higher in the direction parallel to pressing. Therefore, the Young's modulus in the pressing direction in specimens with such a pore texture is smaller than that in the specimens with no such pore texture.

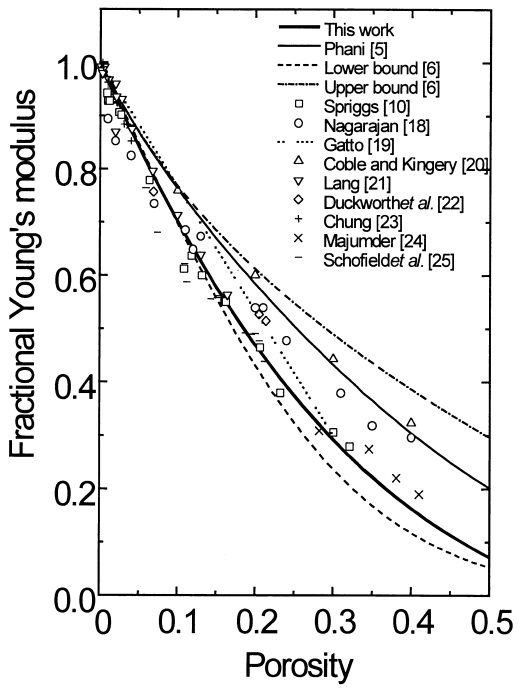

Fig. 4. Effect of the porosity on the Young's modulus of alumina at room temperature.

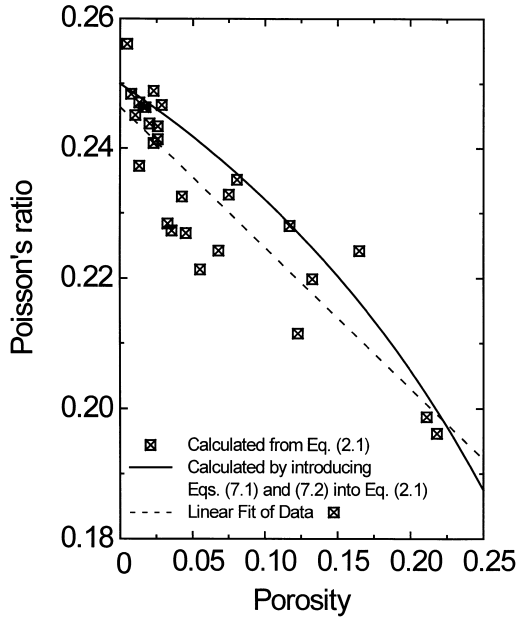

Fig. 5. Calculated Poisson's ratio by the ultrasonic testing plotted against the porosity of alumina.

The Poisson's ratios calculated using Eq. (2.1) are plotted in Fig. 5 as crossed squares, with the dashed line representing the linear fit of these points. The solid curved line shown is calculated by introducing Eqs. (7.1) and (7.2) into Eq. (2.1). Poisson's ratio, similar to Young's modulus, decreases with the increase of the porosity, but with a greater variation [$\nu=\nu_0(1-0.88p)$]. The decrease of the Poisson's ratio indicates that porosity induces a decrease of the strain ratio between strains in directions perpendicular to and parallel to an applied stress, resulting from the above mentioned pore texture.

5. Conclusions

1. The longitudinal and transverse ultrasonic velocities in alumina ceramics decrease approximately proportionally with the increase of the porosity.
2. The linear relationship between the sound velocity and porosity can be qualitatively described by the lowerbound of the model considering cylindrical pores, whereas the model considering spherical pores predicts a smaller value for the porosity factor.
3. The Young's modulus can be predicted from the longitudinal and transverse velocities, which are a function of porosity. The calculated values are in a good agreement with

some of the experimental data that have been obtained from the alumina samples with a uniaxial pore texture.

4. The disagreement between the calculated values and the Young's modulus values reported in other studies is thought to be the result of different forming processes. The uniaxial pressing process produces a preferential pore alignment and results in a smaller Young's modulus in the pressing direction. This is supported by the observation of lower values of the longitudinal velocity, and by decreases in the calculated Poisson's ratio with the porosity.

Acknowledgments

The authors wish to acknowledge that this work was supported by the National Science Council in Taiwan (contract no. NSC79-0210-D002-20).

References

[1] Elligson WA, Roberts RA, Ackerman JL, Sawicka BD, Gronemeyer S, Kritz RJ. Recent developments in nondestructive evaluation for structure ceramics. Int Adv Nondestr Test 1987;13:267–94.

[2] Chang L-S, Chuang T-H. Ultrasonic testing of artificial defects in alumina ceramic. Ceram Int 1997;23:367–73.

[3] Timoshenko SP, Goodier JN. Theory of Elasticity. New York: McGraw-Hill, 1982. pp. 487–90.

[4] Sayers CM. Ultrasonic velocity dispersion in porous materials. J Phys D 1981;14:413–20.

[5] Phani KK. Porosity-dependence of elastic properties and ultrasonic velocity in polycrystalline alumina — a model based on cylindrical pores. J Mater Sci 1996;31:262–6.

[6] Hashin Z, Rosen BW. Elastic moduli of fiber-reinforced materials. J Appl Mech 1964;31:223–32.

[7] Ramakrishnan N, Arunachalam VS. Effective elastic moduli of porous solids. J Mater Sci 1990;25:3930–7.

[8] Kahn M. Acoustic and elastic properties of PZT ceramics and anisotropic pores. J Am Ceram Soc 1985;68:623–8.

[9] Sudduth RD. A generalized model to predict the effect of voids on modulus in ceramics. J Mater Sci 1995;30:4451–62.

[10] Spriggs RM. Expression for effect of porosity on elastic modulus of polycrystalline refractory materials, particularly aluminum oxide. J Am Ceram Soc 1961;44:628–9.

[11] Wang JC. Young's modulus of porous materials: I. Theoretical derivation of modulus–porosity correlation. J Mater Sci 1984;19:801–8.

[12] Phani KK, Niyogi SK. Young's modulus of porous brittle solids. J Mater Sci 1987;22:257–63.

[13] Pennings CM, Grellner W. Precise nondestructive determination of the density of porous ceramics. J Am Ceram Soc 1989;71:1268–79.

[14] Generazio ER, Roth DJ. Ultrasonic imaging of porosity variations produced during sintering. J Am Ceram Soc 1989;72:1282–5.

[15] Spitzig WA, Thompson RB, Jiles DC. Ultrasonic and magnetic analyses of porosity in iron compacts. Metall Trans A 1989;20:571–8.

[16] Bridge B, Round R, Green A. Structural evaluation of phosphate bonded ceramic composite materials from non-destructive ultrasonic velocity and attenuation measurements. J Mater Sci 1991;26:2397–409.

[17] Chai J-F, Wu T-T, Chuang T-H. Primary study of the measurement of porosity in ceramics by ultrasonic testing. Proceeding of Conference on Nondestructive Test. Taipei, 1996. pp. 271–81.

[18] Nagarajan A. Ultrasonic and magnetic analyses of porosity in iron compacts. J Appl Phys 1971;42:3693–6.

[19] Gatto F. Influence of small cavities on velocity of sound in metals. Alluminio 1950;19:19–26.

[20] Coble RL, Kingery WD. Effect of porosity on physical properties of sintered alumina. J Am Ceram Soc 1956;39:377–85.

[21] Lang SM. Properties of high-temperature ceramics and cermets — elasticity and density at room temperature. Natl Bur Stand Monogr 1960;6:45.

[22] Duckworth WH, Johnston JK, Jackson LR, Schofield HZ. Mechanical Properties of Ceramic Bodies, Rand Report No. R-209, Battelle Memorial Institute, Columbus, OH, 1950.

[23] Chung DH. Elastic and Anelastic Properties of Fine-Grained Polycrystalline Alumina at Elevated Temperatures, Bulletin of Research Department, Monthly Report No. 297, State University of New York College of Ceramics at Alfred University, March, 1961.

[24] Majumder BL. Young's modulus of elasticity of ceramic materials by flexure. Trans Indian Ceram Soc 1952;11:168–81.

[25] Schofield HZ, Lynch JF, Duckworth WH. Fundamental Studies of Ceramic Materials, Final Summer Report, Battelle Memorial Institute Report to Office of Naval Research, March 31, 1949.